Proteomic study of differentially expressed proteins in seeds between parents and offspring of castor bean (*Ricinus communis* L.)

Xiaotian Liang[1]; Rui Luo[1]; Yanxin Zhang[1]; Mingda Yin[1]; Yanpeng Wen[1]; Xuemei Hu[1]; Zhiyan Wang[1]; Yumiao Huo[1]; Fenglan Huang[1,2,3,4,5,6]*

[1] College of Life Science and Food Engineering, Inner Mongolia Minzu University, Tongliao, Inner Mongolia, China

[2] Key Laboratory of Castor Breeding of State Ethnic Affairs Commission, Tongliao, Inner Mongolia, China

[3] Research Center for Engineering and Technology of Castor Industry by Universities in Inner Mongolia Autonomous Region, Tongliao, Inner Mongolia, China

[4] Key Laboratory of Castor Breeding of Inner Mongolia Autonomous Region, Tongliao, Inner Mongolia, China

[5] Collaborative Innovation Center of Castor Industry of Inner Mongolia Autonomous Region, Tongliao, Inner Mongolia, China

[6] Engineering Research Center of Castor Industry Technology Innovation, Inner Mongolia Autonomous Region, Tongliao, Inner Mongolia, China

* Corresponding author

E-mail: huangfenglan@imun.edu.cn (FH)

(1973-), female, professor, Ph. D., master's supervisor, engaged in the castor molecular breeding research.

*Fund support

National Natural Science Foundation of China (31860071);

2020 New Agricultural Science Research and Reform Practice Project of the Ministry of Education (2020082);

Inner Mongolia Autonomous Region Grassland Talent Rolling Support Program;

Inner Mongolia Natural Science Foundation General Project (2021MS03008);

Inner Mongolia Autonomous Region Grassland Talent Innovation Team - Castor Molecule Breeding Research Innovative Talent Team Rolling Support Plan;

2021 National Ethnic Affairs Commission Higher Education Teaching Reform Research Project (21082);

Key topics of education and teaching research in Inner Mongolia Minzu University (ZD2020013)

Abstract

Castor bean (*Ricinus communis L.*), one of the top 10 oilseed crops in the world, has high economic value. Hybridization is the most direct and effective method to breed new varieties with high yield, high oil content, and strong stress resistance. Therefore, prediction of desired traits in castor hybrid offspring is particularly important. In this study, proteomic analysis was performed to identify differentially expressed proteins (DEPs) in seeds between castor hybrid offspring and their female (Lm female line aLmAB2) and male parents (CSR•181). Among the DEPs upregulated in the seeds of hybrid offspring, the majority were related to seed yield and stress resistance, while some were related to oil synthesis and fatty acid synthesis and metabolism in seeds. In other words, the hybrid offspring showed heterosis for seed yield, stress resistance, oil synthesis, and fatty acid synthesis and metabolism when compared with their parents. Further, real-time quantitative polymerase chain reaction assays were performed on 12 genes encoding DEPs involved in oil synthesis, pollen abortion, yield, and stress resistance of seeds. The results showed that the expression levels of the 12 genes were consistent with those of the DEPs.

Introduction

Castor bean (*Ricinus communis* L.) belongs to the genus *Ricinus* in the family Euphorbiaceae. Due to its strong environmental adaptability, castor bean can grow in harsh conditions such as saline-alkali soil and heavy metal–contaminated soil and is considered a valuable plant resource for phytoremediation. Therefore, it has been widely planted in tropical, subtropical, and warm temperate countries, especially in India, China, and Brazil [1,2]. China has more than 2300 germplasm resources of castor collected both at home and abroad, and in-depth studies have been conducted to further explore the application of castor bean. In Inner Mongolia, castor bean is a characteristic oilseed crop pivotal to local economic and social development [3]. It is a special industrial oil crop with prominent intraspecific heterosis.

Seed storage substances gradually accumulate during seed development and maturation. Protein, one of the seed storage substances, can help a seed to form cellular structures and provide a nitrogen source for normal metabolism and development of seeds, thereby playing a vital role in cellular structure and function [4]. In 1994, Wilkins and Williams first proposed the concept of the proteome, which refers to all proteins expressed in a cell, tissue, or organism [5]. The methods used for proteomic analysis of seeds mainly include two categories: gel and nongel analysis. Gel analysis is most commonly used, including two-dimensional gel electrophoresis (2-DE) and two-dimensional difference gel electrophoresis (2D-DIGE) [6]. After the differentially expressed spots are determined by using 2-DE and 2D-DIGE, a complete protein atlas can be obtained by mass spectrometry (MS), and this can better

reflect the changes in protein expression and posttranslational modification [7,8]. Proteomic studies of plant seeds have attracted an increasing amount of attention because they can provide information on substance changes in seeds during their growth and development and help explore the adaptative mechanism of plants to environmental stress. Xia et al. [9] conducted proteomic analysis to investigate the impact of temperature on seed metabolism in dormant and germinating seeds and deciphered the regulation of central metabolism activity during seed germination. Gu et al. [10] studied seed germination vigor in *Brassica napus* seeds differing in oil content by an integrated proteomic and genomic approach, and their research laid a foundation for studying the regulatory mechanism of seed germination vigor in *Brassica napus*.

In this study, the seeds from castor female parents (the Lm female line aLmAB2), male parents (CSR•181), and their hybrid offspring were used as the study materials, and the heterotic traits of offspring compared with their parents were identified by proteomic techniques. Further, genes associated with these traits were determined and tested with reverse transcription–quantitative PCR (RT-qPCR). The findings of this study can lay a foundation for guiding the production practice of castor bean and cultivating new castor varieties with high yield, high oil content, and strong stress resistance.

Materials and methods

Experimental materials

Plant materials

The plant materials used in this study were the castor seeds from female parent (aLmAB2), male parent (CSR•181), and their hybrid offspring F_0 and F_1. Castor plants at the flowering stage were bagged and pollinated manually. Subsequently, the seeds that had a developmental time of 20 days (Fig 1A), 40 days (Fig 1B), and 60 days post pollination (DPP) (Fig 1C) were collected. After their testa were removed, the seeds were wrapped in tinfoil paper and stored in an ultralow-temperature freezer at -80°C for subsequent use. The experimental materials were provided by Tongliao Research Institute of Agriculture and Animal Husbandry.

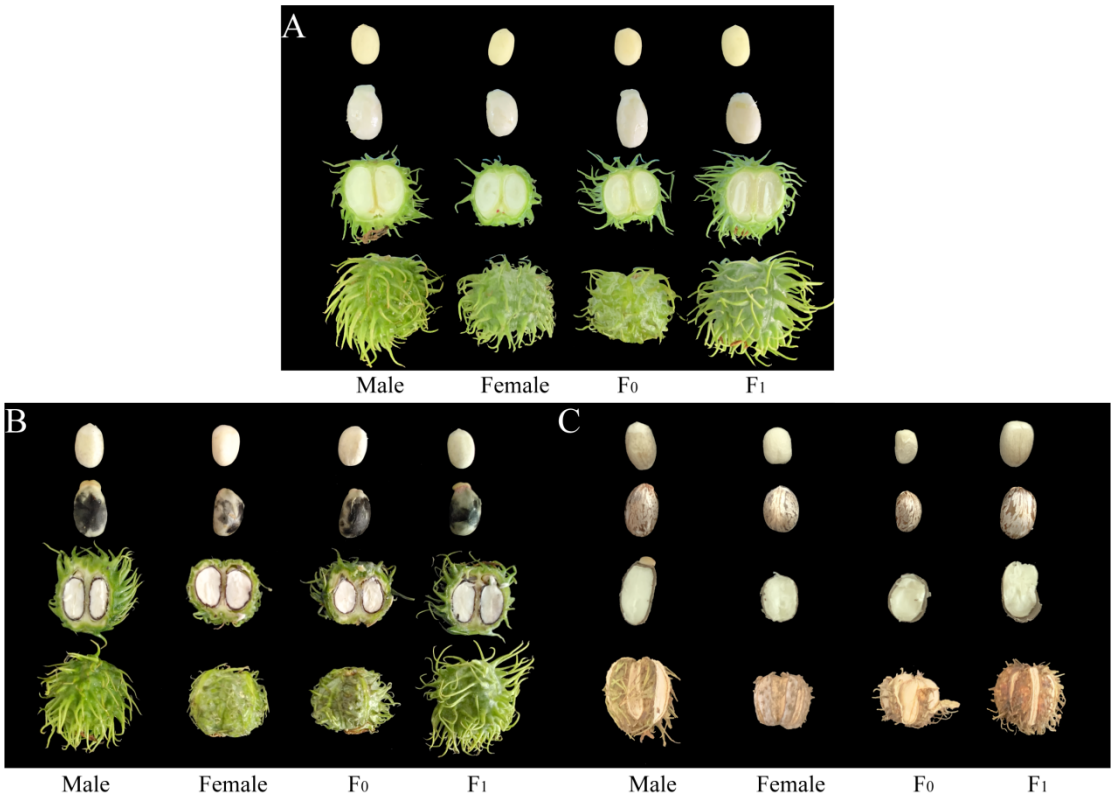

Fig 1. Castor Seeds at Different Developmental Stages.

110 Note: A: 20 DPP; B: 40 DPP; C: 60 DPP

111

112 Reagents and instruments

113 The reagents used in this experiment included Tris-HCI solution, ethylene
114 diamine tetraacetic acid stock solution, 0.4% β-mercaptoethanol solution, 0.9 M
115 sucrose, balanced phenol solution, extraction solution, ammonium acetate/methanol
116 solution, acetone solution, lysis solution, NaOH solution, HCl solution, lysine
117 solution, Amersham CyDye DIGE Fluors (minimal dyes) for the Ettan DIGE kit
118 (GE), the 2-D Clean-up kit (GE), the 2-D Quant kit (GE), hydration solution, 87%
119 glycerol, covering oil, monomer storage solution, 4× separating gel buffer, 10%
120 sodium dodecyl sulfate (SDS) solution, N,N,N′,N′-tetramethylethylenediamine
121 (TEMED), 10% ammonium persulfate solution, 75% alcohol, gel-sealing liquid,
122 equilibrium solution, bromophenol blue dye, 1,4-dithiothreitol (DTT), iodoacetamide
123 (IAA), premixed protein marker, SDS electrophoresis buffer, stationary liquid,
124 amplification solution, Coomassie brilliant blue dye, decolorizing solution, RNA
125 Rapid Extraction Kit for plants (ZOMANBIO), GoTaq® qPCR and RT-qPCR
126 Systems (Promega), and reverse transcription system (Promega). All reagent formulas
127 are shown in S1 Table. The instruments used in this study included high-speed and
128 low-speed refrigerated centrifuges (Thermo), an Infinite M200 Pro multifunctional
129 microplate reader (TECAN), a gel imaging system and electrophoresis apparatus
130 (Bio-Rad), the Ettan IPGphor 3 for electrophoresis by isoelectric focusing (IEF) in the
131 first dimension, a MultiTemp IV water bath, a FLA9500 multifunctional biomolecular

132 imager (GE), and a real-time fluorescence-based quantitative PCR system (ABI 7500,
133 ABI company).
134

135 2-DE

136

137 Sample preparation

138 An optimized phenol extraction method was used to extract protein from
139 castor seeds. The obtained dry protein powder was aliquoted into 1.5-mL centrifuge
140 tubes. Each tube was added with a 20-fold volume of lysis solution (each 1 mL of
141 lysis solution was added to 0.0062 g DTT, 20 μL of immobilized pH gradient (IPG)
142 buffer, and 40 μL of protease inhibitor before use). Then, the tube was vortexed at a
143 low temperature for 30 minutes, followed by an ultrasound ice-bath for 20 minutes.
144 The process was repeated until dry protein powder was fully dissolved. After
145 centrifugation at 13,000*g* for 1 hour at 4 °C, the supernatant was transferred to a
146 1.5-mL centrifuge tube. The 2-D Clean-up kit was used to remove impurity from the
147 sample. The 2-D Quant kit was used for sample quantitation, which derived a
148 standard curve: $y = -0.0041x + 0.3751$ ($R^2 = 0.999$), where y was the absorbance
149 value of the postquantitation sample at 480 nm and x was the protein concentration
150 (μg/μL).
151

152 2-DE procedures

153 For the first dimension, 450 μL of the sample solution containing 800 μg of
154 protein was loaded for electrophoresis by IEF. First, 800 μg of the lysed sample was
155 transferred into a centrifuge tube, which was then added to hydration solution to
156 achieve a total volume of 450 μL (each 1 mL of hydration solution was added with 5
157 μL of NL3-10 IPG buffer and 0.0028 g of DTT). Then, the sample solution was
158 vacuum-centrifuged at 13,000 rpm for 1 hour at 4 °C. After the centrifuged sample
159 solution was transferred to the strip groove, a 24-cm-long dry gel strip (pH 3-10 NL)
160 was placed into the groove; after ensuring that the gel surface was fully in contact
161 with the sample, the covering oil was added, and then a lid was placed to cover the gel
162 strip groove. Finally, after all gel strips of samples had been placed into a PROTEAN
163 IEF instrument, the following IEF protocol was run the Table 1 at a constant
164 temperature of 20 °C:

165 **Table 1. IEF Program.**

Program	Voltage/V	Time/h	Purpose
S1	30	8	Hydration
S2	50	4	Desalination
S3	100	1	Desalination
S4	300	1	Desalination
S5	600	1	Desalination
S6	1000	2	Desalination
S7	8000	12	Focusing
S8	1000	∞	Maintaining

166 For the second-dimension SDS-PAGE, 12.5%T polyacrylamide gel was used.
167 First, the gel strips after the first-dimension IEF were equilibrated for 15 minutes in

168 each of 2% (w/v) DTT and 2.5% (w/v) IAA equilibration buffer. Then the
169 well-equilibrated strips were sealed with sealing liquid in a gel plate, which was then
170 placed in the Ettan DALT 12 unit (12 gels per run) (GE-061-TY7119, GE
171 Healthcare). Electrophoresis was performed at 2 W per gel for 1 hour and then 16 W
172 per gel until the bromophenol blue band was 0.5-1 cm away from the bottom of the
173 gel.

174 After electrophoresis, the gel was taken out and sequentially submerged in
175 stationary liquid for 30 minutes, amplification solution for 20 minutes, Coomassie
176 brilliant blue dye for 10 minutes, and finally the decolorizing solution until only
177 protein spots appeared on the gel, without other, interfering dye residues. The Image
178 Scanner III image scanning system (28-9076-07 GE Healthcare, USA) was used for
179 gel imaging, and the Image Master 2-D Platinum 7.0 software was used for gel image
180 analysis.

181

182 # 2D-DIGE

183

184 ## Sample preparation

185 The sample was lysed using the lysis solution without DTT or IPG buffer.
186 After lysis, the sample solution was adjusted to pH 8.0-9.0 using 100 mM NaOH and
187 1 M HCl, with a target pH of 8.5. The subsequent procedures were the same as those
188 described in 1.2.1.

189

190 ## Preparation of CyDye DIGE fluor minimal dyes

191 Preparation of 1 nmol/μL fluorescent dye stock solution: After the dye-storing
192 tube was taken out of the -80°C refrigerator, each tube received 5 μL of
193 *N*,*N*-dimethylformamide solution and then vortexed for 30 seconds to fully dissolve
194 the dye. Next, it was centrifuged at 12,000*g* for 30 seconds to push the dye stock
195 solution to the bottom of the tube. Preparation of 400 pmol/μL fluorescent dye
196 working solution: Five microliters of fluorescent dye stock solution was diluted with
197 7.5 μL of *N*,*N*-dimethylformamide solution to achieve a final concentration of 400
198 pmol/μL, followed by centrifugation at 12,000*g* for 30 seconds to push the solution to
199 the bottom of the tube. All the above procedures were performed at 4 °C in the dark.

200 A certain volume of the sample solution (containing 50 μg of protein) was
201 taken out and mixed with 1 μL of the dye working solution through vortexing,
202 followed by a brief centrifugation. Then, as a quench-labeling reaction, the sample
203 was kept on ice in the dark for 30 minutes and then mixed with 1 μL of 10 mM lysine
204 solution through vortexing. After a brief centrifugation, the sample was placed on ice
205 in the dark for 10 minutes.

206

207 ## 2D-DIGE procedures

208 According to the experimental design, the internal standard sample and the
209 target samples labeled with Cy2, Cy3, or Cy5 were mixed in a centrifuge tube and
210 then added to hydration solution (every 1 mL of hydration solution had been added
211 with 5 μL of NL3-10 IPG buffer and 0.0028 g of DTT) up to a total volume of 450

212 μL. After being placed on ice in the dark for 10 minutes, the sample solution was
213 treated as in 1.2.2 for the first-dimension IEF.

214 For the second-dimension SDS-PAGE, 12.5% polyacrylamide gel was
215 prepared using low-fluorescence glass plates, followed by the same procedures as in
216 1.2.2. Light exposure was avoided during the entire process. The Typhoon FLA9500
217 multifunctional biomolecular imager was used for gel imaging, and the DeCyder
218 software for 2D-DIGE analysis was used to identify and annotate the differentially
219 expressed spots (ratio ≥ 1.5 and ANOVA ≤ 0.05).

220

221 # MS identification and analysis of the DEP spots

222

223 ## MS identification

224 The DEP spots in the gel were recovered and sent to Shanghai Bioclouds
225 Biological Tech Co. Ltd. for MS identification.

226

227 ## Database search and functional classification of differentially
228 expressed proteins (DEPs)

229 The information of the DEPs identified by MS were obtained by searching the
230 database of castor bean proteins (https://www.ncbi.nlm.nih.gov/). The proteins were
231 functionally classified into Gene Ontology (GO) categories according to UniProt
232 (http://www.UniProt.org/) and QuickGO (https://www.ebi.ac.uk/QuickGO/), and their

233 roles in metabolic pathways were categorized according to the Kyoto Encyclopedia of
234 Genes and Genomes (KEGG) Pathway Database (https://www.kegg.jp/kegg/pathway.
235 html). The histograms of GO classification were generated on the Omics Cloud
236 platform established by GENE DENOVO (http://www.omicshare.com/index.php).
237 The heatmaps were drawn using GraphPad Prism7.04 software.
238

239 RT-qPCR verification

240 The RNA Rapid Extraction Kit for plants was used to extract RNA from
241 castor seeds. The extracted RNA was reverse-transcribed into cDNA. SnapGene 2.8.0
242 software was used to design primers (Table 2).

243 **Table 2. RT-qPCR Primer Sequences.**

Spot No.	Name	Primer sequence (5′-3′)	Tm (°C)
A2	A2F	CAGGCTATCGCAAATGGTGAC	56.6
	A2R	ACAGGTGCAAGATTCTTCCAG	54.9
A9	A9F	CAAGTCAGGCCAATCAAGCAC	56.4
	A9R	ACAAGCTCGCCAACTTTGAC	56.8
A10	A10F	GCATCCTCAAGGAAGAGTTGC	56.4
	A10R	TGTTGCCGACAAGGTATGGT	56.7
A13	A13F	CAGGCCATCTTGCAGCATTG	57.6
	A13R	AGAGACAGTCATGACACGGTG	56.8
J1	J1F	TTCCACCAATGGCCAGTACC	57.8
	J1R	GGAGGCATGAAAGGCTTCTTG	56.7
B5	B5F	TCAGAGCTTCAGAGCTGGTG	57.1
	B5R	CGTGTTGGCCTGTTTCATAGG	56.6
B9	B9F	TCATGGAGTTTGCTTGTACTCG	54.8
	B9R	AGATAGGAGCAGCATTGTTTCC	54.8

B12	B12F	TGAGGCGAAACGTGATGTCAG	57.8
	B12R	CGGTTCGAGGTCTAGTCTTCTC	56.8
K15	K15F	GCCACAGGCTAATGAAGTTCG	56.6
	K15R	ACACCAGGACCAACACTCTC	57.1
K4	K4F	GGTGCACAGATGTTGCAGTC	57.1
	K4R	TCCTGGAGACAAAGTGGTGAG	56.7
K13	K13F	GAGGAAGGACTTGAGCTCCTG	57.7
	K13R	ATTGCTGGAGTTGCTGGC	56.4
N5	N5F	AGCATAATGCCATGCATGTCC	56.0
	N5R	AGGTTCCATTTCCTCGTGGC	58.0

The GoTaq® qPCR systems was used for qPCR. The reaction system consisted of 10 μL of SYBR Premix Ex *Taq*, 0.4 μL of Rox reference dye II, 1.0 μL of each of the upstream and downstream primers, 2.0 μL of template DNA, and ddH_2O up to 20 μL. The amplification program was by 45 cycles of 95°C for 30 seconds (s), 95°C 10 s, melting temperature for 45 s, and 72 °C for 10 s. The results were calculated using the $2^{-\Delta\Delta Ct}$ method.

One-way ANOVA was performed with SPSS version 19.0 software, and the relevant histograms were generated in Excel 2019 software.

Results

Optimization of the 2-DE system

Optimization of conditions for 2-DE

258 To determine whether it is necessary to remove impurities from protein
259 samples in this experiment, the same protein samples were divided into two groups,
260 one with impurity removal and the other without impurity removal, before 2-DE
261 (24-cm dry gel strips, pH 3-10 NL, protein loading amount 800 μg). The results are
262 presented in S1 Fig. To determine the optimal pH range for this experiment, the
263 protein samples with the same treatment (with or without impurity removal) were
264 subjected to IEF and SDS-PAGE using the 24-cm dry gel strips with pH 3-10 NL or
265 pH 4-7. The results are shown in S2 Fig. To determine the optimal protein loading
266 amount, different amounts of protein (800 μg, 1000 μg, and 1200 μg) were loaded for
267 2-DE (24-cm dry gel strips; pH 3-10 NL) under the same conditions. The comparison
268 results are shown in S3 Fig. Based on the results of these preliminary experiments, the
269 optimal experimental conditions were impurity removal, 24-cm dry gel strips with pH
270 3-10 NL, and a loading amount of 800 μg. These conditions were used in the
271 following experiments.
272

273 2D-DIGE results

274 The castor seeds at different developmental stages from parents and offspring
275 were subjected to 2D-DIGE. The results are shown in Fig 2.

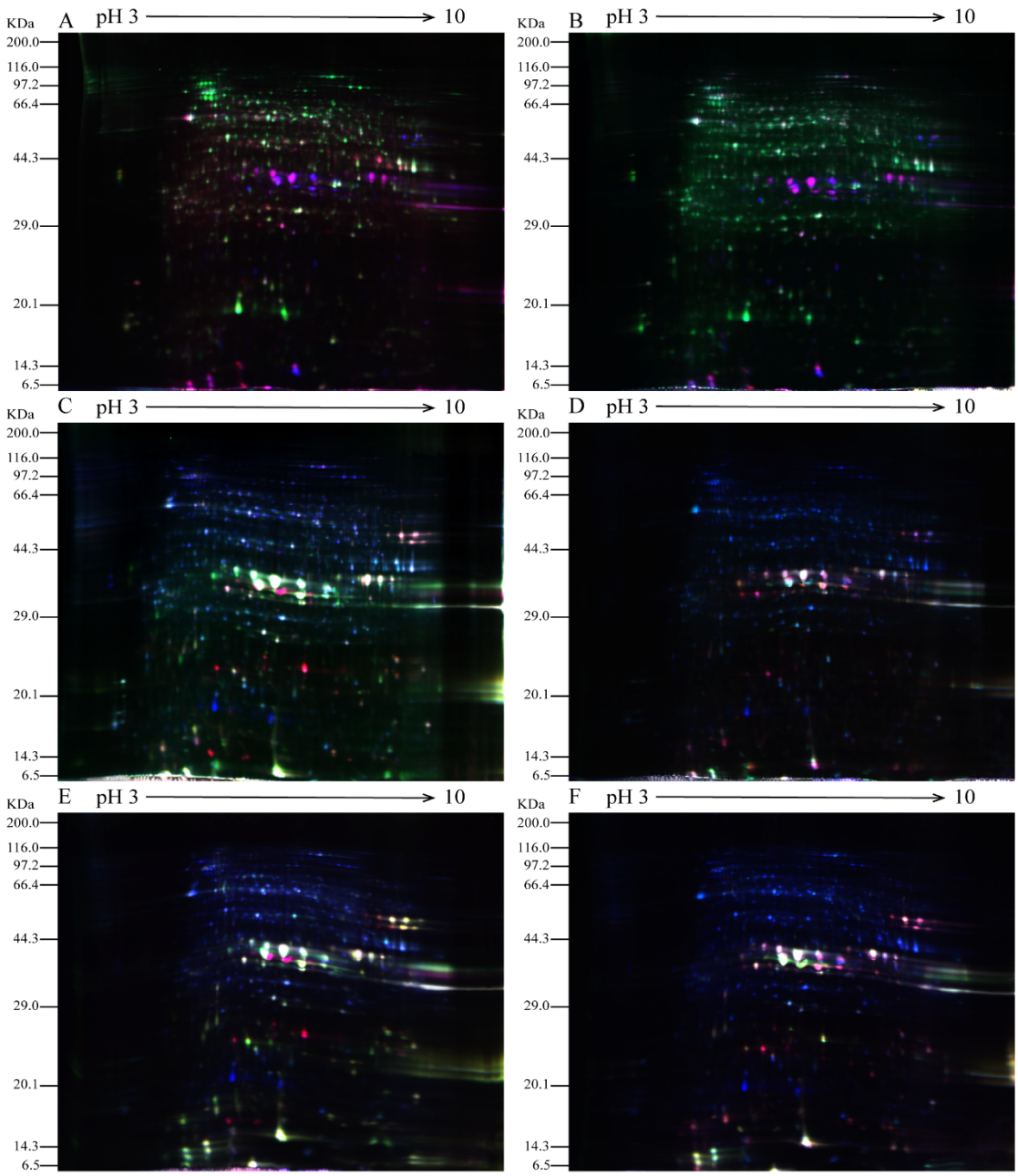

Fig 2. 2D-DIGE Results of Castor Parents and their Offspring

Note: A: Male, F_0, 20 d. B: Female, F_1, 20 d, A&B when they had Developed to 20 DPP. C: Male, F_0, 40 d. D: Female, F_1, 40 d, C&D when they had Developed to 40 DPP. E: Male, F_0, 60 d. F: Female, F_1, 60 d, E&F when they had Developed to 40 DPP.

In the figures, the blue protein spots denote the internal standard samples labeled with Cy2; the green protein spots are the Cy3-labeled samples from male and

284 female parents; and the red protein spots are the Cy5-labeled samples from castor
285 offspring. In Fig 2, the 2D-DIGE protein spots for the seeds at different development
286 stages from both castor parents and offspring indicate that the dye labeling of all three
287 samples was successful and met the requirements for experimental analysis.
288

289 MS identification and functional classification results of 290 DEPs

291

292 MS identification results

293 The 2D-DIGE results of castor seeds at different development stages from
294 parents and their offspring were analyzed for differences using DeCyder 2-D
295 software. A total of 122 differentially expressed spots (ratio ≥ 1.5 and ANOVA ≤
296 0.05) were determined and recovered, of which 121 spots containing 93 proteins were
297 successfully identified by matrix-assisted laser desorption/ionization mass
298 spectrometry (MALDI-TOF-MS). The results are shown in S2 Table. The
299 sources/names and classification of these DEPs are listed in S3 Table. Among the
300 DEPs between the castor parents and their offspring, 69 were present in seeds at 20
301 DPP, 46 in seeds at 40 DPP, and 20 in seeds at 60 DPP. Some proteins had a
302 significantly different expression in the castor seeds at two or all three development
303 stages between castor parents and their offspring, such as starch synthase, D-7 late
304 embryogenesis abundant (LEA) protein, superoxide dismutase (SOD), and aspartic
305 proteases (APs).

306

307 **Functional classification results of the DEPs**

308 The 93 DEPs identified were classified to five categories (Fig 3) related to
309 stress responses (61.29%), seed nutrient storage (17.20%), fatty acid synthesis and
310 metabolism (12.90%), amino acid metabolism (6.45%), and others (2.15%). The
311 DEPs were most often related to stress responses. These included SOD, APs, D-7
312 LEA protein, and glutathione peroxidase. The DEPs associated with nutrient storage
313 in seeds included starch synthase (chloroplast/starch), 2S albumin precursor, and
314 vicilin GC72-A. The DEPs associated with fatty acid synthesis and metabolism
315 included stearoyl-ACP desaturase, oil body–associated protein 2C (OBAP2C), and
316 acetyl-CoA carboxylase. The DEPs associated with amino acid metabolism included
317 transaldolase, transketolase (chloroplast), S-adenosylmethionine synthase (SAMS),
318 and others.

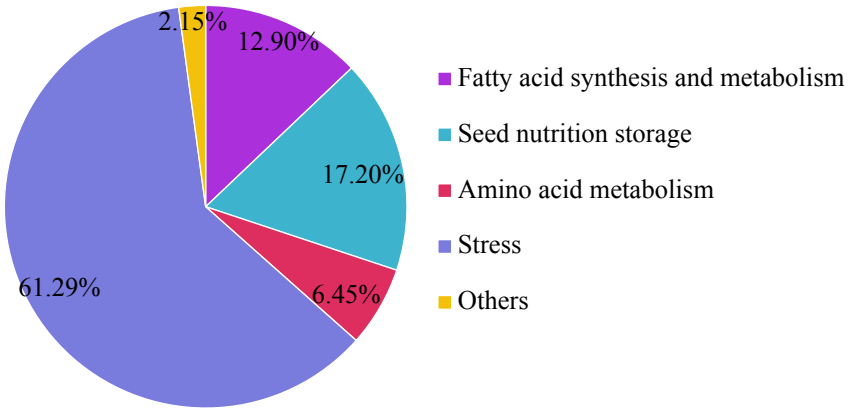

319

320 **Fig 3. Functional Classification of the Differentially Expressed Proteins between**
321 **Castor Parents and their Offspring.**

322 ***Functional classification results of the DEPs in seeds at 20 DPP***
323 ***between castor parents and their offspring***

324 A total of 69 DEPs were identified in seeds at 20 DPP between castor parents
325 and their offspring. The seeds from F_1 offspring had 16 upregulated DEPs (e.g.,
326 OBAP2C, acetyl transferase NATA1, and 2S albumin precursor) when compared with
327 their male parent and 13 upregulated DEPs (e.g., protein disulfide isomerase (PDI),
328 luminal-binding protein 5, and triphosphate isomerase) when compared with their
329 female parent. The seeds from F_1 offspring had 23 downregulated DEPs (e.g.,
330 dihydrolipoyl dehydrogenase 1, MLP-like protein 34, and salicylic acid-binding
331 protein 2) when compared with their male parent and nine downregulated DEPs (e.g.,
332 l-ascorbate peroxidase, adenosine kinase 2, and the 36-kDa porin in mitochondrial
333 outer membrane) when compared with their female parent. In the F_0 seeds, 11 DEPs
334 (e.g., legume protein A, SOD, and hydroxyl-ACP dehydrase) were upregulated when
335 compared with their male parent, and five DEPs (i.e., transaldolase, stearoyl-ACP
336 desaturase, 60S acidic ribosomal protein P2, SOD, and uncharacterized protein) were
337 upregulated when compared with their female parent. The F_0 seeds had 11
338 downregulated DEPs (e.g., the major latex allergen Hev b5, MLP-like protein 31, and
339 GDP-mannose 3,5-epimerase 1) when compared with their male parent and four
340 downregulated DEPs (i.e., adenosyl homocysteinase, xylem serine proteinase 1
341 precursor, cytochrome *c* oxidase subunit 6b-1, and lactoylglutathione lyase GLX1)
342 when compared with their female parent. The relative expression levels of DEPs are
343 shown in S4 Fig, and the results regarding their involvement in KEGG metabolic
344 pathways are shown in S5 Fig.

345 Fig 4 shows the GO functional annotations of the 69 DEPs in the three
346 categories of biological process, cellular component, and molecular function. The
347 DEPs between F_1 and parents and DEPs between F_0 and parents were mostly
348 associated with biological processes, including starch synthase, ribulose bisphosphate
349 carboxylase small chain, and glutathione peroxidase. A smaller number of DEPs were
350 associated with molecular functions, including glutathione peroxidase, APs, and
351 acetyltransferase NATA1. The fewest DEPs were associated with cellular
352 components, including 60S acidic ribosomal protein P2, stearoyl-ACP desaturase, and
353 PDI. The analysis of KEGG metabolic pathways showed that the DEPs between F_1
354 and parents and the DEPs between F_0 and parents were mostly involved in rcu01100
355 (metabolic pathways) and rcu01110 (biosynthesis of secondary metabolites), such as
356 alcohol dehydrogenase 1 (ADH1), starch synthase, and hydroxyl-ACP dehydrase. A
357 number of DEPs were involved in rcu01230 (biosynthesis of amino acids), rcu00710
358 (carbon fixation in photosynthetic organisms), and rcu00061(fatty acid biosynthesis).

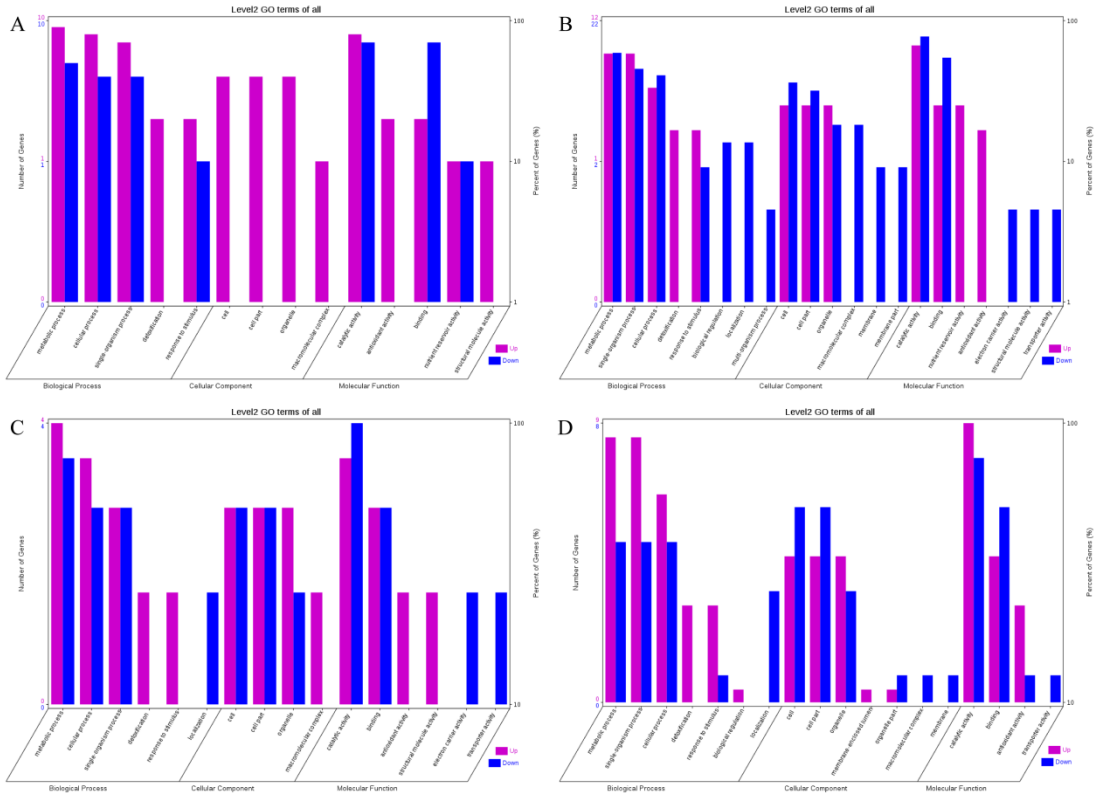

Fig 4. GO Functional Annotation of Differentially Expressed Proteins in Seeds at 20 DPP between Castor Parents and their Offspring.

Note: A: Male, F_1, 20 DPP; B: Female, F_1, 20 DPP, C: Male, F_0, 20 DPP; D: Female, F_0, 20 DPP.

Functional classification results of the DEPs in seeds at 40 DPP between castor parents and their offspring

A total of 46 DEPs were identified in seeds at 40 DPP between castor parents and their offspring. The F_1 seeds had three upregulated DEPs when compared with their male parent, including D-7 LEA protein, legume protein A, and heat shock protein (HSP); and they had 10 upregulated DEPs when compared with their female parent, including the large subunit of 2S sulfur-rich seed storage protein, nucleolar

372 protein 56 (NOP56), and reduced nicotinamide adenine dinucleotide phosphate
373 (NADPH)-dependent aldehyde reductase 1. Compared with their male parents, four
374 DEPs were downregulated in the F_1 seeds, including ATP synthase subunit β, HSP,
375 ADH1, and plastid 3-keto-acyl-ACP synthase; when compared with female parents,
376 six DEPs were downregulated, including starch synthase, fructose-bisphosphate
377 aldolase, GroES chaperonin, etc. In the F_0 seeds, seven DEPs (e.g., APs, large
378 subunits of 2S sulfur-rich seed storage protein, and nucleoside diphosphate kinase
379 (NDPK)) and nine DEPs (e.g., SOD, D-7 LEA protein, and glutelin type-A precursor)
380 were upregulated when compared with the male and female parents, respectively. One
381 DEP (enoyl-ACP reductase (EAR) precursor) and three DEPs (i.e.,
382 translation-controlled tumor protein homolog, pre-pro-ricin, and GroES chaperonin)
383 were downregulated when compared with the male and female parents, respectively.
384 Compared with the F_0 generation, the seeds of the F_1 generation had seven
385 upregulated DEPs (e.g., legume protein A, HSP, and 14-3-3-like protein D isoform
386 X1) and seven downregulated DEPs (e.g., fructose-bisphosphate aldolase 1, adenosine
387 kinase 2, and adenosyl homocysteinase). The relative expression levels of the DEPs
388 mentioned above are depicted in S6 Fig, and the results regarding their involvement in
389 the KEGG metabolic pathways are presented in S7 Fig.

390 The GO functional annotations for the 46 DEPs are presented in Fig 5. The
391 majority of DEPs in seeds between F_1 and male parent were related to biological
392 processes and molecular functions; compared with the male parent, only legume
393 protein A was upregulated while all other DEPs were downregulated in the F_1 seeds.

394 Most of the DEPs in seeds between F_1 and the female parent (e.g., NADPH-dependent
395 aldehyde reductase 1 and rRNA N-glycosidase) were associated with biological
396 processes and molecular functions. Similarly, most of the DEPs between F_0 and
397 parents were related to biological processes and molecular functions, including
398 cysteine protease inhibitor and glutelin type-A precursor. The DEPs between F_1 and
399 F_0 were mostly related to biological processes, including SAMS and adenosyl
400 homocysteinase; the DEP categorized under cellular component was enolase, and
401 those categorized under molecular function included HSP and 14-3-3-like protein D
402 isoform X1. According to the KEGG metabolic pathways, some HSP family members
403 involved in rcu04141 (protein processing in endoplasmic reticulum), including HSP,
404 were differentially expressed in seeds between F_1 and parents, between F_0 and
405 parents, and between F_1 and F_0. In addition, among the upregulated DEPs in the F_0
406 seeds vs. the male parent, NDPK was involved in rcu04016 (MAPK signaling
407 pathway) and betaine aldehyde dehydrogenase 1 (BADH1) was involved in rcu00260
408 (glycine, serine, and threonine metabolism). SOD, an upregulated DEP in the F_0 seeds
409 compared with their female parent, was involved in rcu04146 (peroxisome); and
410 chaperonin, an upregulated DEP in the F_1 generation compared with F_0, was involved
411 in rcu03018 (RNA degradation).

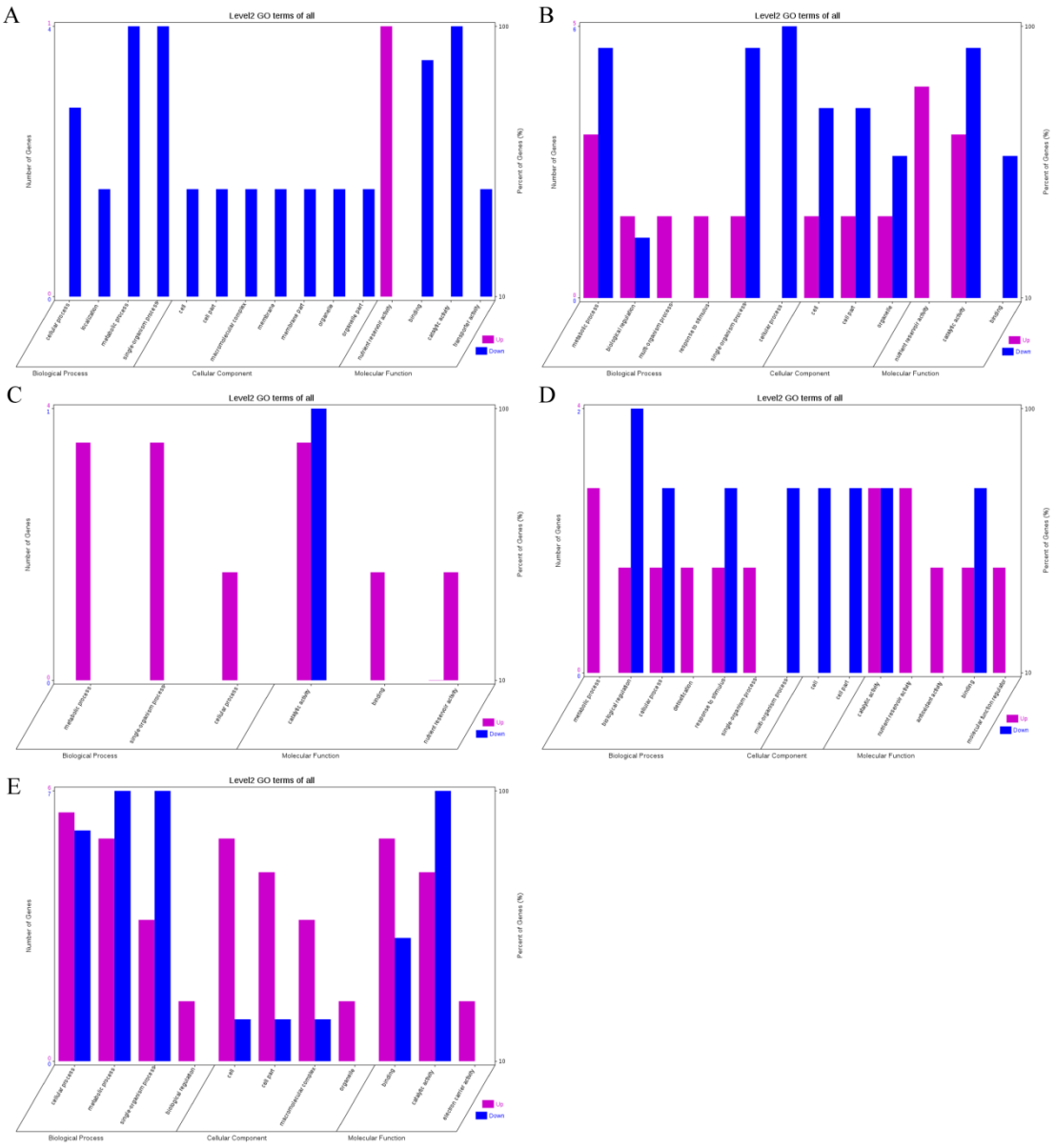

Fig 5. GO Functional Annotation of Differentially Expressed Proteins in Seeds at 40 DPP between Castor Parents and their Offspring.

Note: A: Male, F_1, 40 DPP; B: Female, F_1, 40 DPP; C: Male, F_0, 40 DPP; D: Female, F_0, 40 DPP; E: F_1 vs. F_0, 40 DPP.

Functional classification results of the DEPs in seeds at 60 DPP between castor parents and their offspring

420 A total of 25 DEPs were identified in seeds at 60 DPP between castor parents
421 and their offspring. The F_1 seeds had two upregulated DEPs when compared with
422 their male parent, NOP56 and 5-methyltetrahydroproylglutamate-homocysteine
423 methyltransferase; and they had six upregulated DEPs when compared with their
424 female parent, including D-7 LEA protein, NDPK, and large subunits of
425 ribulose-1,5-bisphosphate carboxylase/oxygenase. Five DEPs were downregulated in
426 the F_1 seeds compared with their male parent, including malate dehydrogenase,
427 phospho-glucosidase, and enolase, and no DEP showed detectable downregulation in
428 expression in the F_1 seeds compared to their female parent. In the seeds of the F_0
429 generation, three DEPs (i.e., vicilin GC72-A, legume protein A, and seed storage
430 protein) and eight DEPs (e.g., 6-phosphogluconate dehydrogenase, large subunits of
431 2S sulfur-rich seed storage protein, and D-7 LEA protein) were upregulated compared
432 to the male and female parents, respectively. No DEP showed detectable
433 downregulation in the F_0 seeds compared with either of their parents. Compared with
434 F_0, the F_1 seeds had five upregulated DEPs (e.g., 2S albumin precursor,
435 phospho-glucosidase, and malate dehydrogenase) but no downregulated DEP. The
436 relative expression levels of the abovementioned DEPs are shown in S8 Fig, and the
437 results on their involvement in KEGG metabolic pathways are shown in S9 Fig. The
438 DEPs between F_0 and the male parent were not involved in any metabolic pathways.
439 The GO functional annotations of the 25 DEPs are shown in Fig 6. Most of the
440 DEPs between F_1 and parents and between F_0 and parents (e.g., ADH1, NOP56, and
441 NDPK) were related to biological processes and molecular functions. Most of the

442 DEPs between F_1 and F_0 (e.g., phospho-glucosidase, malate dehydrogenase, and
443 enolase) were related to biological processes. From the KEGG metabolic pathway
444 analysis, the DEPs between F_1 and parents, between F_0 and parents, and between F_1
445 and F_0 were mostly involved in rcu01100 (metabolic pathways) and rcu01110
446 (biosynthesis of secondary metabolites), including 6-phosphogluconate
447 dehydrogenase, ADH1, and 5-methyltetrahydroproylglutamate-homocysteine
448 methyltransferase. In addition, the DEPs upregulated in F_1 and F_0 over their parents
449 were also involved in the pathways of rcu00270 (cysteine and methionine
450 metabolism), rcu00592 (alpha-Linolenic acid metabolism), rcu00230 (purine
451 metabolism), etc. The DEPs upregulated in the F1 generation compared with F0 also
452 participated in the pathways related to rcu01200 (carbon metabolism) and rcu01230
453 (biosynthesis of amino acids).

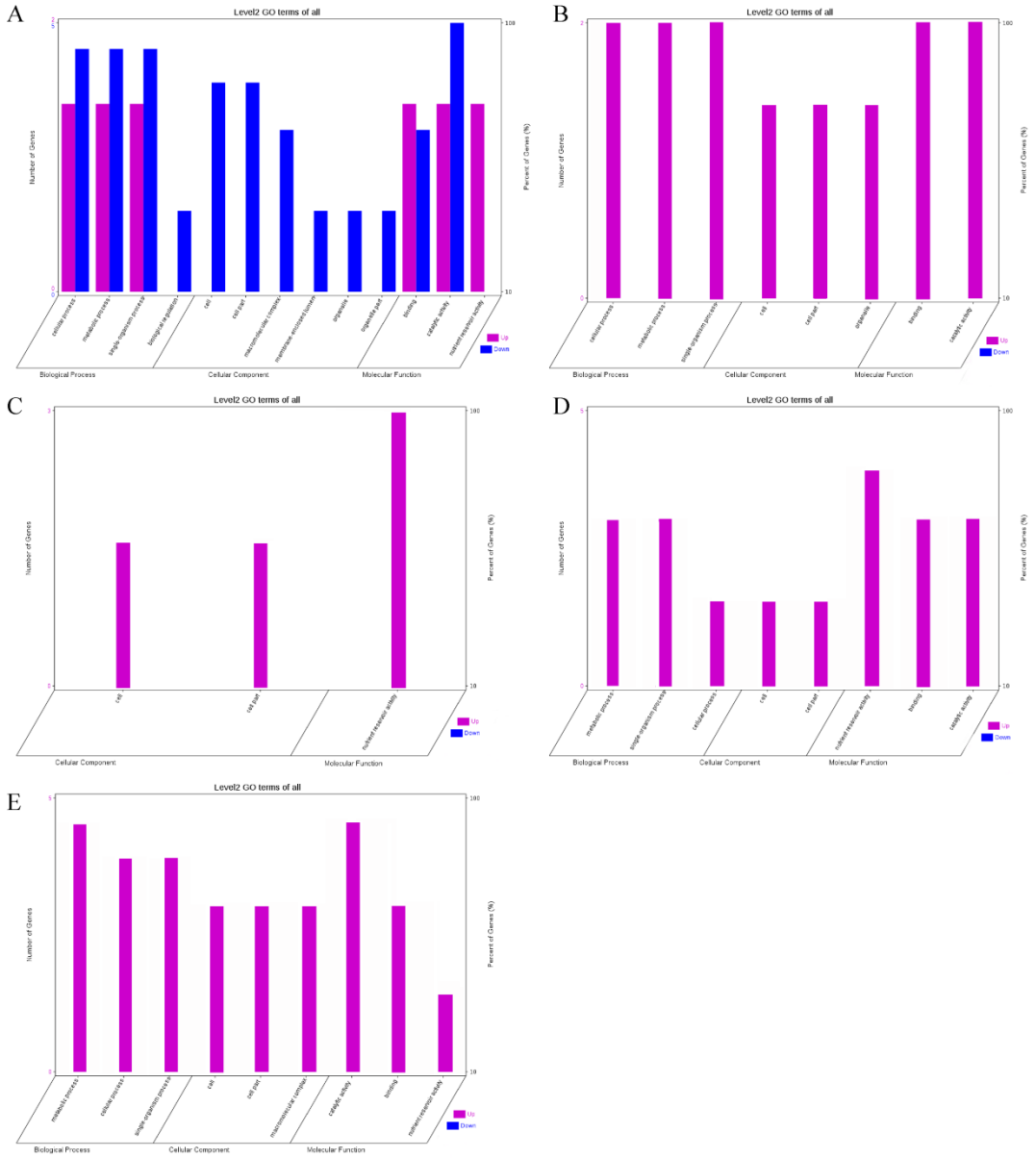

Fig. 8-1. GO Ffunctional Aannotation of Ddifferentially Eexpressed Pproteins in Sseeds at 60 DPP between Ccastor Pparents and their Ooffspring.

Note: A: Male, F1, 60 DPP; B: Female, F1, 60 DPP; C: Male, F0, 60 DPP; D: Female, F0, 60d; E: F1 vs. F0, 60 DPP.

RT-qPCR results of the DEPs

Twelve DEPs in the seeds between castor parents and their offspring (Table 3) were selected for RT-qPCR analysis, and the results are shown in Fig 9. The

463 expression of the genes corresponding to the 12 DEPs all showed differences

464 consistent with those of the DEPs.

465 **Table 3. The 12 Differentially Expressed Proteins Chosen for RT-qPCR**

466 **Analysis.**

Spot No.	Protein Name	Source	Time (d)	Related Traits
J1	Stearoyl ACP desaturase	F_0 Male	20	Oil synthesis Amino acid metabolism
K4	Oil body associated protein 2C	F_1 Male	20	Oil synthesis Amino acid metabolism
B12	Acetyl-CoA carboxylase	F_1 Female	20	Oil synthesis Amino acid metabolism
A10	26S protease regulatory subunit 6a	F_1 Male	20	Pollen abortion
N5	Cysteine protease	F_1 Male	20	Pollen abortion
A2	Superoxide dismutase	F_0 Female	40	Yield and stress resistance
A13	Amylosynthetase	F_1 Male	20	Yield and stress resistance
B5	Abundant protein D-7 in late embryonic development	F_1 Male	20	Yield and stress resistance
B9	Glutathione peroxidase	F_1 Male	20	Yield and stress resistance
K15	Alcohol dehydrogenase 1	F_1 Female	60	Yield and stress resistance
K13	2S albumin precursor	F_1 Male	20	Yield and stress resistance
A9	Aspartic protease	F_1 Male	20	Yield and stress resistance

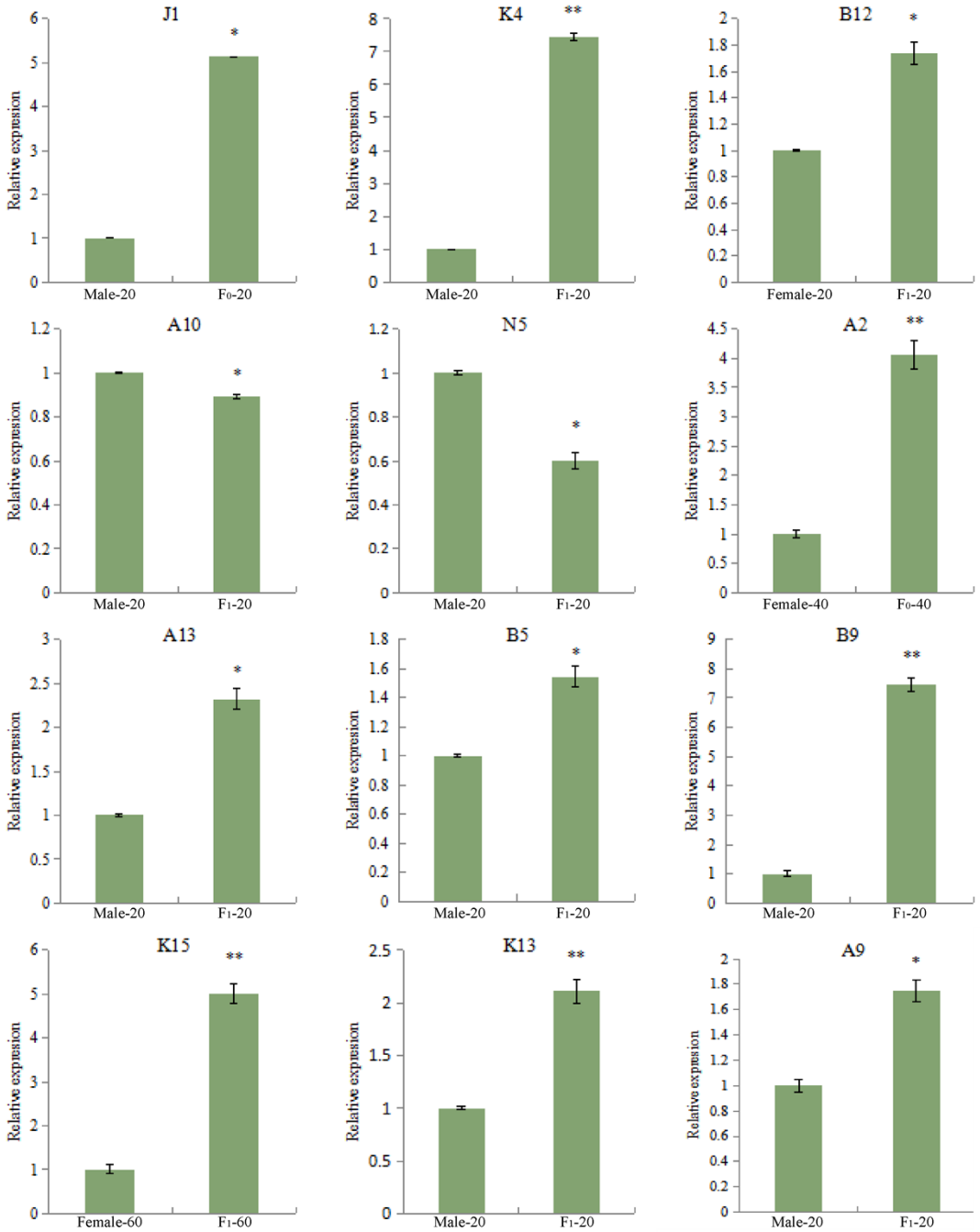

Fig 7. The RT-qPCR Results of Partially Differentially Expressed Proteins between Castor Parents and their Offspring.

Note: *: 0.01<P≤0.05, **: 0<P≤0.01.

Discussion

473 Through comparative proteomic analysis of seeds at different developmental
474 stages between castor parents and their offspring, 122 DEP spots were detected by
475 MS, though they only contained 93 DEPs. This is because a number of proteins were
476 significantly differentially expressed at all developmental stages of seeds, such as
477 starch synthase, D-7 LEA protein, SOD, and APs.

478 Most of the DEPs were associated with stress responses (61.29%) and they
479 were mostly upregulated in the seeds of offspring, which was consistent with the
480 results of physiological and biochemical measurements. SOD is an antioxidant
481 enzyme in the reactive oxygen species scavenging system that effectively prevents
482 peroxides (e.g., H_2O_2) from damaging the structure and function of plant cells. This
483 enzyme participates in the rcu04146 pathway (peroxisome). The peroxisome, an
484 essential organelle of plants, plays a key role in redox signal transduction and lipid
485 homeostasis [11-15]. APs are mainly involved in such processes as metabolism,
486 precursor protein processing, protein degradation, and programmed cell death, as well
487 as pollen germination and pollen-tube growth in plants [16-18]. D-7 LEA is a
488 stress-responding protein that massively accumulates in the late embryonic stage and
489 is generated under adverse conditions such as drought. It regulates the metabolic
490 balance of plants through mechanisms such as stabilizing the cell membrane and
491 binding metal ions [19-21]. Glutathione peroxidase contains sulfhydryl groups and
492 can effectively block the free radicals of reactive oxygen species from further
493 damaging the body by scavenging H_2O_2 and lipid peroxides [22,23]. ADH1, a
494 medium-chain zinc-containing enzyme widely found in various tissues in plants,

binds zinc ions. Zinc plays an essential role in the synthesis of indole-3-acetic acid (IAA), an auxin in plants. Zinc deficiency can lead to decreased tryptophan and IAA content, hindering the growth of plant roots. Therefore, ADHs are is closely related to plant growth and development [24-26]. In addition to those five proteins, several DEPs between offspring and parents were associated with stress responses, including 14-3-3-like protein, BADH1 (chloroplast), and l-ascorbate peroxidase.

Among the DEPs between castor offspring and parents, 17.20% were involved in seed nutrient storage, most of which were upregulated in the offspring seeds. Starch synthase is a key enzyme involved in starch synthesis and metabolism. Starch, the main storage carbohydrate, may account for 50% of the dry matter in storage organs (tubers or seeds), and it is an important energy source for plant growth and development, so its content directly determines the yield of crops [27-29]. 2S albumin precursor, a storage protein, can gradually be degraded to produce various amino acids and thereby provide essential nitrogen, carbon, and sulfur sources for plant growth during the seed germination and early growth stages, which is of great significance for plant growth and development [30]. Vicilin GC72-A belongs to the family of antimicrobial peptides, a class of small-molecule polypeptides synthesized by plants to defend against pathogen invasion; these antimicrobial peptides can inhibit or kill a variety of microorganisms and fungi [31,32]. Other DEPs associated with seed nutrient storage of plants included adenosyl homocysteinase, NOP56, and salicylic acid-binding protein 2.

516 Among the DEPs between castor offspring and parents, 12.90% was related to
517 plant fatty acid synthesis and metabolism, most of which were upregulated in the
518 offspring seeds. This result was consistent with the results of trait and quality
519 assessment. Stearoyl-ACP desaturase is a key enzyme in the conversion between
520 stearic acid and unsaturated fatty acids, so its upregulation may increase the
521 unsaturated fatty acid content in plants, thereby improving their resistance to low
522 temperature [33]. OBAP2C plays an essential role in the seed development of plants.
523 The oil body, a lipid-storing subcellular organellar particle in plant seeds, provides
524 nutrients to plants and is critical for plant growth and development [34-36].
525 Acetyl-CoA carboxylase is a biotinidase catalyzing the carboxylation of acetyl-CoA
526 to form malonyl-CoA in the initial step of fatty acid synthesis. Fatty acids re
527 membrane lipid components of all cells and an important energy reserve of
528 multicellular organisms. Hence, acetyl-CoA carboxylase, the catalyzer of the first step
529 of fatty acid biosynthesis, plays a critical role in plant growth and development
530 [37-39]. Other DEPs associated with fatty acid synthesis and metabolism included
531 EAR precursor, plastid 3-keto-acyl-ACP synthase I, and hydroxyl-ACP dehydrase.

532 Only 6.45% of the DEPs between castor offspring and parents were related to
533 amino acid metabolism, most of which were upregulated in the offspring seeds. Both
534 transaldolase and transketolase (chloroplast) are enzymes involved in the
535 nonoxidative phase of the pentose phosphate pathway. Transaldolase catalyzes the
536 transfer of the dihydroxyacetone moiety from sedoheptulose-7-phosphate to
537 glyceraldehyde-3-phosphate; as a result, it can regulate the production of

538 ribose-5-phosphate and NADPH by the pentose phosphate pathway, through which it
539 links the pentose phosphate shunt and glycolysis pathways and regulates the balance
540 between the oxidative and nonoxidative phases of the pentose phosphate pathway.
541 Transketolase is a "nonregulatory" enzyme that catalyzes the reversible transfer of
542 aldehyde group from activated ketose (donor) to activated aldose (receiver). The
543 upregulation of transketolase expression facilitates carbon fixation in plants, as well
544 as plant growth and development [40-44]. SAMS is the only enzyme synthesizing
545 SAM in organisms. SAM, a metabolite from the interaction of methionine and
546 adenosine triphosphate, has been widely found in animals, plants, and
547 microorganisms. It is involved in up to 40 types of biochemical reactions and plays a
548 significant role in improving the drought resistance of plants [45-48]. All three
549 enzymes mentioned above were involved in rcu01230 (biosynthesis of amino acids).
550 In addition, NADP-dependent isocitrate dehydrogenase, l,l-diaminopimelate
551 aminotransferase (chloroplast), and 5-methyltetrahydroproylglutamate-homocysteine
552 methyltransferase in the amino acid biosynthesis pathway were also differentially
553 expressed in seeds between castor offspring and parents.

554 The high expression of cysteine protease and 26S protease regulatory subunit
555 6a can lead to abnormal degradation of some regulatory proteins in anther tissue and
556 cause pollen abortion. In this study, these two proteins were downregulated in F_1
557 compared with their male parent [49]. Importantly, we found that cysteine protease
558 inhibitor was upregulated in the offspring seeds compared with their parents. This
559 enzyme can bind to cysteine protease to inhibit its activity and reduce the risk of

560 pollen abortion, and it is involved in the stress responses of plants under adverse
561 conditions and participates in physiological processes such as senescence of plants
562 [50].
563

564 # Conclusions

565 To conduct a proteomic analysis to compare the differences in castor seeds at
566 different developmental stages between parents and their offspring, we first optimized
567 our two-dimensional electrophoresis system. The protein atlas obtained from
568 SDS-PAGE following IEF was the best when using samples after impurity removal,
569 24-cm dry gel strips (pH 3-10 NL), and a protein loading amount of 800 μg.

570 By 2D-DIGE analysis under these optimal two-dimensional electrophoresis,
571 93 DEPs were identified in the seeds at different developmental stages between castor
572 parents and offspring. They belonged to five categories: proteins related to stress
573 response (61.29%), seed nutrient storage (17.20%), fatty acid synthesis and
574 metabolism (12.90%), amino acid metabolism (6.45%), and others (2.15%).

575 RT-qPCR was performed on 12 DEPs, including 1) stearoyl-ACP desaturase,
576 OBAP2C, and acetyl-CoA carboxylase, which were upregulated in the offspring seeds
577 compared with their parents and are involved in oil synthesis and fatty acid synthesis
578 and metabolism; 2) 26S protease regulatory subunit 6a and cysteine protease, which
579 were downregulated in the offspring seeds compared with their parents and are
580 involved in pollen abortion; and 3) SOD, starch synthase, D-7 LEA protein,
581 glutathione peroxidase, ADH1, 2S albumin precursor, and APs, which were

582 upregulated in the offspring seeds compared with their parents and are involved in
583 plant resistance to adverse conditions. The RT-qPCR results showed that the
584 expression levels of the genes encoding these 12 DEPs were consistent with the
585 expression of the DEPs.

586 In summary, this study can help guide the production of castor beans and lays
587 the foundation for cultivating new castor varieties with high yield, high oil content,
588 and strong stress resistance.

589

590 # References

591 1. Yu A, Li F, Liu A. Comparative proteomic and transcriptomic analyses
592 provide new insight into the formation of seed size in castor bean. BMC Plant
593 Biol. 2020;20: 48.

594 2. Olivares AR, Carrillo-González R, González-Chávez MdCA, Soto Hernández
595 RM. Potential of castor bean (Ricinus communis L.) for phytoremediation of
596 mine tailings and oil production. J Environ Management. 2013;114: 316-323.

597 3. Peng M, Xiao-Hua Z, Feng-Lan H, et al. Effect of different treatments on
598 seeds germination of castor. Heilongjiang Agricultural Sciences. 2012.

599 4. Zhu MM, Liu EQ, Bao Y, Duan SL, She J, Liu H, et al. Low concentration of
600 corn steep liquor promotes seed germination, plant growth, biomass
601 production and flowering in soybean. Plant Growth Regul. 2019;87: 29-37.

602 5. Iimure T, Sato K. Beer proteomics analysis for beer quality control and
603 malting barley breeding. Food Res Int. 2013;54: 1013-1020.

604 6. Kim ST, Kim SG, Agrawal GK, Kikuchi S, Rakwal R. Rice proteomics: a
605 model system for crop improvement and food security. Proteomics. 2014;14:
606 593-610.
607 7. Sghaier-Hammami B, Castillejo MÁ, Baazaoui N, Jorrín-Novo JV, Escandón
608 M. GeLC-Orbitrap/MS and 2-DE-MALDI-TOF/TOF comparative proteomics
609 analysis of seed cotyledons from the non-orthodox Quercus ilex tree species. J
610 Proteom. 2021;233: 104087.
611 8. Jian M, Zhang D, Wang X, Wei S, Zhao Y, Ding Q, et al. Differential
612 expression pattern of the proteome in response to cadmium stress based on
613 proteomics analysis of wheat roots. BMC Genom. 2020;21: 343-343.
614 9. Xia Q, Ponnaiah M, Cueff G, Rajjou L, Prodhomme D, Gibon Y, et al.
615 Integrating proteomics and enzymatic profiling to decipher seed metabolism
616 affected by temperature in seed dormancy and germination. Plant Sci.
617 2018;269: 118-125.
618 10. Gu J, Hou D, Li Y, Chao H, Zhang K, Wang H, et al. Integration of proteomic
619 and genomic approaches to dissect seed germination vigor in Brassica napus
620 seeds differing in oil content. BMC Plant Biol. 2019;19: 21.
621 11. Azarabadi S, Abdollahi H, Torabi M, Salehi Z, Nasiri J. ROS generation,
622 oxidative burst and dynamic expression profiles of ROS-scavenging enzymes
623 of superoxide dismutase (SOD), catalase (CAT) and ascorbate peroxidase
624 (APX) in response to Erwinia amylovora in pear (Pyrus communis L). Eur J
625 Plant Pathol. 2016;147: 279-294.

626 12. Lu BW, An FX, Cao LJ, Yang YJ, Liu PM, Wang X, et al. Proteomic profiling
627 uncovered the cytosolic superoxide dismutase BsSOD1 associated with plant
628 defence in the herbal orchid Bletilla striata. Funct Plant Biol. 2020;47: 937.
629 13. Jafari S, Garmdareh SEH, Azadegan B. Effects of drought stress on
630 morphological, physiological, and biochemical characteristics of stock plant
631 (Matthiola incana L.). Sci Hortic. 2019;253: 128-133.
632 14. Pour-Aboughadareh A, Etminan A, Abdelrahman M, Siddique KHM, Tran
633 LSP. Assessment of biochemical and physiological parameters of durum
634 wheat genotypes at the seedling stage during polyethylene glycol-induced
635 water stress. Plant Growth Regul. 2020;92: 81-93.
636 15. Che Y, Zhang N, Zhu X, Li S, Wang S, Si H. Enhanced tolerance of the
637 transgenic potato plants overexpressing Cu/Zn superoxide dismutase to low
638 temperature. Sci Hortic. 2020;261: 108949.
639 16. Soares A, Carlton SMR, Simões I. Atypical and nucellin-like aspartic
640 proteases: emerging players in plant developmental processes and stress
641 responses. J Exp Bot. 2019;70: 2059-2076.
642 17. Yang Y, Feng D. Genome-wide identification of the aspartic protease gene
643 family and their response under powdery mildew stress in wheat. Mol Biol
644 Rep. 2020;47: 8949-8961.
645 18. Sebastián DI, Fernando FD, Raúl DG, Gabriela GM. Overexpression of
646 Arabidopsis aspartic protease APA1 gene confers drought tolerance. Plant Sci.
647 2020;292: 110406.

648 19. Park SC, Kim YH, Jeong JC, Kim CY, Lee HS, Bang JW, et al. Sweetpotato
649 late embryogenesis abundant 14 (IbLEA14) gene influences lignification and
650 increases osmotic- and salt stress-tolerance of transgenic calli. Planta.
651 2011;233: 621-634.
652 20. Li N, Zhang S, Liang Y, Qi Y, Chen J, Zhu W, et al. Label-free quantitative
653 proteomic analysis of drought stress-responsive late embryogenesis abundant
654 proteins in the seedling leaves of two wheat (Triticum aestivum L.) genotypes.
655 J Proteom. 2018;172: 122-142.
656 21. Zhao W, Yao F, Zhang M, Jing T, Zhang S, Hou L, et al. The potential roles
657 of the G1LEA and G3LEA proteins in early embryo development and in
658 response to low temperature and high salinity in artemia sinica. PLoS One.
659 2016;11: e0162272.
660 22. Eshdat Y, Holland D, Faltin Z, Ben-Hayyim G. Plant glutathione peroxidases.
661 Physiol Plant. 1997;100: 234-240.
662 23. Kammoun M, Essid MF, Ksouri F, Rokka V-M, Charfeddine M,
663 Gargouri-Bouzid R, et al. Assessment of physiological age and antioxidant
664 status of new somatic hybrid potato seeds during extended cold storage. J
665 Plant Physiol. 2020;254: 153279.
666 24. Kim YH, Huh GH. Overexpression of cinnamyl alcohol dehydrogenase gene
667 from sweetpotato enhances oxidative stress tolerance in transgenic
668 Arabidopsis. Vitro Cell Dev Biol Plant. 2019;55: 172-179.

669 25. Zhuang M, Lam SK, Zhang J, Li H, Shan N, Yuan Y, et al. Effect of full
670 substituting compound fertilizer with different organic manure on reactive
671 nitrogen losses and crop productivity in intensive vegetable production system
672 of China. J Environ Manag. 2019;243: 381-384.
673 26. Rattanapolsan L, Nakbanpote W, Sangdee A. Zinc- and cadmium-tolerant
674 endophytic bacteria from Murdannia spectabilis (Kurz) Faden. studied for
675 plant growth-promoting properties, in vitro inoculation, and antagonism. Arch
676 Microbiol. 2020;203: 1131-1148.
677 27. Wang CL, Zhang ZP, Miao MM. SNF1-related protein kinase (SnRK) 1
678 involved in the regulation of raffinose family oligosaccharide metabolism in
679 cucumber (Cucumis sativus L.) Calli. J Plant Growth Regul. 2016;35:
680 851-864.
681 28. Mehrpouyan S, Menon U, Tetlow IJ, Emes MJ. Protein phosphorylation
682 regulates maize endosperm starch synthase IIa activity and protein−protein
683 interactions. Plant J. 2021;105: 1098-1112.
684 29. do Carmo CD, Sousa MB, Brito AC, de Oliveira EJ. Genome-wide association
685 studies for waxy starch in cassava. Euphytica. 2020;216: 82.
686 30. Nguyen TP, Cueff G, Hegedus DD, Rajjou L, Bentsink L. A role for seed
687 storage proteins in Arabidopsis seed longevity. J Exp Bot. 2015;66:
688 6399-6413.
689 31. Lopes FES, da Costa HPS, Souza PFN, Oliveira JPB, Ramos MV, Freire JEC,
690 et al. Peptide from thaumatin plant protein exhibits selective anticandidal

691 activity by inducing apoptosis via membrane receptor. Phytochemistry.
692 2019;159: 46-55.
693 32. Wang C, Yang C, Gao C, Wang Y. Cloning and expression analysis of 14
694 lipid transfer protein genes from Tamarix hispida responding to different
695 abiotic stresses. Tree Physiol. 2009;29: 1607-1619.
696 33. Whittle EJ, Cai Y, Keereetaweep J, Chai J, Buist PH, Shanklin J. Castor
697 stearoyl-ACP desaturase can synthesize a vicinal diol by dioxygenase
698 chemistry. Plant Physiol. 2020;182: 730-738.
699 34. de Oliveira TS, Freitas-Silva O, Kluczkovski AM, Campelo PH. Potential use
700 of vegetable proteins to reduce Brazil nut oil oxidation in microparticle
701 systems. Food Res Int. 2020;137: 109526.
702 35. Zhou LZ, Chen FS, Hao LH, Du Y, Liu C. Peanut oil body composition and
703 stability. J Food Sci. 2019;84: 2812-2819.
704 36. Jolivet P, Acevedo F, Boulard C, d'Andréa S, Faure J-D, Kohli A, et al. Crop
705 seed oil bodies: from challenges in protein identification to an emerging
706 picture of the oil body proteome. Proteomics. 2013;13: 1836-1849.
707 37. Parvy JP, Napal L, Rubin T, Poidevin M, Perrin L, Wicker-Thomas C, et al.
708 Drosophila melanogaster Acetyl-CoA-carboxylase sustains a fatty
709 acid-dependent remote signal to waterproof the respiratory system. PLoS
710 Genet. 2012;8: e1002925.
711 38. Vijayakumar A, Olson I, Wang T, Hollenback D, Toteva M, Trevaskis J, et al.
712 Efficacy and safety of an acetyl CoA carboxylase inhibitor are improved in

713 combination with PPAR agonists in a dyslipidemic rat model. J Hepatol.
714 2020;73: S656.
715 39. Thelen JJ, Ohlrogge JB. Both antisense and sense expression of biotin
716 carboxyl carrier protein isoform 2 inactivates the plastid acetyl-coenzyme A
717 carboxylase inArabidopsis thaliana. Plant J. 2002;32: 419-431.
718 40. Oaks Z, Jimah J, Grossman CC, Beckford M, Kelly R, Banerjee S, et al.
719 Transaldolase haploinsufficiency in subjects with acetaminophen-induced
720 liver failure. J Inherit Metab Dis. 2020;43: 496-506.
721 41. Zheng M, Zhu C, Yang T, Qian J, Hsu Y-F. GSM2, a transaldolase,
722 contributes to reactive oxygen species homeostasis in Arabidopsis. Plant Mol
723 Biol. 2020;104: 39-53.
724 42. Tylki-Szymanska A, Wamelink MMC, Stradomska TJ, Salomons GS, Taybert
725 J, Dąbrowska-Leonik N, et al. Clinical and molecular characteristics of two
726 transaldolase-deficient patients. Eur J Pediatr. 2014;173: 1679-1682.
727 43. Li M, Zhang X, Lu Y, Meng S, Quan H, Hou P, et al. The nuclear
728 translocation of transketolase inhibits the farnesoid receptor expression by
729 promoting the binding of HDAC3 to FXR promoter in hepatocellular
730 carcinoma cell lines. Cell Death Dis. 2020;11: 31.
731 44. Bi H, Li F, Wang H, Ai X. Overexpression of transketolase gene promotes
732 chilling tolerance by increasing the activities of photosynthetic enzymes,
733 alleviating oxidative damage and stabilizing cell structure in Cucumis sativus
734 L. Physiol Plant. 2019;167: 502-515.

735 45. Seong ES, Jeon MR, Choi JH, Yoo JH, Lee JG, Na JK, et al. Overexpression
736 of S-Adenosylmethionine synthetase enhances tolerance to cold stress in
737 Tobacco. Russ J Plant Physiol. 2020;67: 242-249.
738 46. Mo HJ, Sun YX, Zhu XL, Wang XF, Zhang Y, Yang J, et al. Cotton
739 S-adenosylmethionine decarboxylase-mediated spermine biosynthesis is
740 required for salicylic acid- and leucine-correlated signaling in the defense
741 response to Verticillium dahliae. Planta. 2016;243: 1023-1039.
742 47. Elango R. Methionine nutrition and metabolism: insights from animal studies
743 to inform human nutrition. J Nutr. 2020;150: 2518S-2523S.
744 48. Kovács L, Mendel Á, Szentgyörgyi A, Fekete S, Söre F, Posta K, et al.
745 Comparative analysis of overexpressed Fragaria vesca
746 S-adenosyl-l-methionine synthase (FvSAMS) and decarboxylase (FvSAMDC)
747 during salt stress in transgenic Nicotiana benthamiana. Plant Growth Regul.
748 2020;91: 53-73.
749 49. Passarge A, Demir F, Green K, Depotter JRL, Scott B, Huesgen PF, et al. Host
750 apoplastic cysteine protease activity is suppressed during the mutualistic
751 association of Lolium perenne and Epichloë festucae. J Exp Bot. 2021;72:
752 3410-3426.
753 50. Kaur H, Gill RS, Kaur S. Rice bean (Vigna umbellata Thunb. Ohwi and
754 Ohashi) protection against Callosobruchus maculatus F.” by presence of
755 protein profile. J Stored Prod Res. 2020;86: 101574.